ROYAL SOCIETY
OF CHEMISTRY

Dynamics of fluorinated imide-based ionic liquids using nuclear magnetic resonance techniques†

Tawhid Pranto,[ab] Carla C. Fraenza, [iD] ‡*[c] Frederik Philippi, [iD] [d] Daniel Rauber, [iD] [e] Christopher W. M. Kay, [iD] [ef] Tom Welton, [iD] [d] Steven G. Greenbaum [iD] [ac] and Sophia Suarez [iD] *[ab]

There is increasing interest in studying molecular motions in ionic liquids to gain better insights into their transport properties and to expand their applications. In this study, we have employed the fast field cycling relaxometry and pulsed field gradient nuclear magnetic resonance techniques to investigate the rotational and translational dynamics of fluorinated imide-based ionic liquids (ILs) at different temperatures. We have studied a total of six ILs composed of the 1-butyl-3-methylimidazolium cation ([BMIM]$^+$) combined with chemically modified analogs of the bis((trifluoromethyl)sulfonyl)imide anion ([NTf$_2$]$^-$ or [TFSI]$^-$). The primary objective of this paper is to broaden the understanding of how the anion's conformational flexibility, fluorination, and mass affect the molecular dynamics of cations and anions. Our results indicate that flexibility has the most significant impact on the rotational and translational motions of ions. Meanwhile, the effect of fluorination and mass is only relevant when conformational flexibility does not change significantly between the ILs being compared.

Introduction

Ionic liquids (ILs) are liquids that consist exclusively of ions. They possess a wide range of useful properties such as low to zero flammability due to negligible vapor pressure, high chemical and thermal stability, a broad liquid-state temperature window, a wide electrochemical voltage window ($\sim$2–6 V), fairly good ionic conductivity ($\sim$1–10 mS cm^{-1}) and a broad polar to non-polar solubility range.[1,2]

ILs have proven to be promising candidates as electrolytes for high-performance batteries when partnered with an appropriate lithium salt.[3–9] Currently, lithium-ion batteries use flammable carbonate solvents as electrolyte components, which has created safety concerns for their rigorous applications, limiting their development and commercialization in large-scale applications such as automotive and storage of energy from

renewable sources. Hence, the research spotlight is shifting increasingly towards developing and studying novel materials like alternative electrolytes that can provide insights into how to mitigate or minimize these safety concerns.[8,10–12] However, ILs generally have relatively high viscosity[2,13,14] compared to their organic solvent counterparts, which slows down transport properties such as ionic conductivity or diffusion. Therefore, it represents a significant drawback to their practical applicability as electrolytes. Thus, a better understanding of how different factors can influence the ILs' viscosity or transport properties is crucial for developing ILs with low viscosity.

Since many properties of ILs are affected by viscosity, its exploration can serve as a reference. In fact, transport parameters such as the self-diffusion of ions, and therefore the IL's viscosity, are affected by ion size, molecular mass and the shape of ions, the magnitude of interaction between cations and anions and conformational flexibility.[15] Specifically, fluorination and conformational flexibility of the anion can affect the IL's viscosity, whereas the influence of mass is less significant.[16] A clear example of this is the weakly interacting anion bis((trifluoromethyl)sulfonyl)imide ([NTf$_2$]$^-$ or [TFSI]$^-$) that is widely studied in the literature,[17–22] which in general forms a low viscosity IL due to low energy barriers for rotation around the S–N bonds that cause high conformational freedom.[23,24] Additionally, due to its high degree of fluorination, the negative charge is effectively delocalized over the whole molecular ion, thereby reducing the ion's coordination affinity and basicity. Among the most popular cations that are used to lower viscosity is 1-butyl-3-methylimidazolium ([BMIM]$^+$)[17,18,20,25]

[a] *Department of Physics, The Graduate Center of CUNY, New York, NY, USA*

[b] *Department of Physics, Brooklyn College of CUNY, New York, NY, USA. E-mail: snsuarez@brooklyn.cuny.edu*

[c] *Department of Physics & Astronomy, Hunter College of CUNY, New York, NY, USA. E-mail: carla.cecilia.fraenza@unc.edu.ar*

[d] *Department of Chemistry, Molecular Sciences Research Hub, Imperial College London, London, UK*

[e] *Department of Chemistry, Saarland University, Saarbrücken, Germany*

[f] *London Centre for Nanotechnology, University College London, London, UK*

† Electronic supplementary information (ESI) available. See DOI: https://doi.org/10.1039/d4cp03166k

‡ Present address: IFEG-CONICET and National University of Cordoba, Cordoba, Argentina.

2462 | *Phys. Chem. Chem. Phys.*, 2025, **27**, 2462–2472

This journal is © the Owner Societies 2025

with its relatively short and flexible alkyl chain which partially shields the positive charge and reduces the Coulomb interactions with the anions.[26]

In this work, we study the rotational and translational dynamics of fluorinated imide-based ILs using nuclear magnetic resonance (NMR) techniques. This is an extension of a previous study[16] which demonstrated that the viscosity of fluorinated imide-based ILs can be optimized by tuning the chemical structure of their anions, and that conformational flexibility is an essential factor to design ILs with low viscosity. The previous study engendered targeted modifications of the [TFSI]⁻ anion. The objective of our study is to broaden our understanding of how the anion's conformational flexibility, fluorination, and mass affect the molecular dynamics of cations and anions. To do this, we used fast field cycling (FFC) relaxometry and pulsed field gradient (PFG) NMR techniques to gain insight into the ion motions on a molecular level over a wide timescale (typically 10^{-3} to 10^{-9} s).

While both techniques have provided valuable information for the characterization of ionic liquids, by comparison, FFC-NMR[27–29] is the lesser used technique due to its inability to provide site-specific information (chemical shift). Despite this, the ability of FFC to sweep frequencies offers the benefit of accessing spectral density functions which depend mainly on the Larmor frequency and the correlation (translational and rotational) times. In the last decade, FFC has been applied to imidazolium-based ILs,[17,18,20,25,30–37] as well as others.[21,38–40] Damodaran[41] recently presented a more comprehensive review on the use of NMR techniques, particularly FFC-NMR, in the study of dynamics in ILs. A few noteworthy examples of the application of FFC NMR to study ILs include the work of Seyedlar et al.[32] who studied the ¹H FFC dispersion profiles for alkyl methylimidazolium bromide ILs over the temperature range of 294–351 K. Their results showed two main features: weakening of the dispersion at elevated temperatures, and more pronounced frequency dependence at lower temperatures. These features have also been observed for other ILs and have been attributed to the dependence of ion–ion interactions and dynamics on temperatures. Another example is the 1-ethyl-3-methylimidazolium (EMIM) triflate ionic liquid study by Wencka et al.[35] using variable temperature ¹H and ¹⁹F FFC relaxometry. Their results showed that both rotational and translational diffusional processes controlled the dynamics.

On the other hand, molecular dynamics simulations have been used to investigate how the structure, shape, and mass of the anion,[42,43] along with the conformational flexibility of the cation,[44] influence the ion dynamics in ILs. However, there is still limited exploration in the literature regarding the various factors that affect both the translational and rotational dynamics of ions.

In this paper, six ILs composed of the [BMIM]⁺ cation combined with chemically modified analogs of the [TFSI]⁻ anion were investigated. They differ in mass, structure, conformational dynamics, and viscosity, all of which are variables for discussion and are known influencers of ion dynamics. To the best of our knowledge, this is the first study that combines the PFG and FFC NMR techniques to isolate the effect of mass, fluorination level, and conformational flexibility of the anion and viscosity on rotational and translational dynamics of the ions in imide-based ionic liquids.

Theory

Fast field cycling (FFC) NMR relaxometry is a powerful tool to investigate the molecular dynamics of a substance or a complex material.[27–29,45] It is a noninvasive low-field, low-resolution NMR technique that provides the dependence of the longitudinal relaxation time T_1, or relaxation rate $R_1 = 1/T_1$, on the strength of the external magnetic field B_0 (or Larmor frequency $\omega_0 = \gamma B_0$, where γ is the nuclear gyromagnetic ratio) and this is called relaxation dispersion profile. It is important to note that this technique cannot distinguish NMR signals from different chemical groups or molecules with the same type of nucleus. Consequently, the T_1 values are average values rather than site-specific.

In this study, the ¹H and ¹⁹F relaxation dispersion profiles of the ILs were analyzed by considering translational diffusion and molecular rotations as the main relaxation mechanisms commonly considered in liquids.[46] The force-free-hard-sphere (FFHS) model was used to describe the translational diffusion contribution, which assumes normal diffusion of a rigid sphere; the molecules are uniformly distributed outside the distance of the closest approach, d, and spins are at the center of the molecules.[47,48] If it is assumed that diffusion is described by finite jumps that meet the Brownian limit $r^2/6d^2 \to 0$, where r^2 is the mean square jump distance defined by $r^2 \equiv 6D\tau$, D is the diffusion constant and τ is the mean time between jumps, the following equations can be deduced for the homonuclear (¹H–¹H or ¹⁹F–¹⁹F) and heteronuclear (¹H–¹⁹F) translational relaxation rates, $R_{1\text{Diff}}$:[46,49]

$$R^{ii}_{1\text{Diff}}(\omega_i) = \frac{A^{ii}_{\text{D}}}{d_{ii}D_{ii}}\left[\tilde{J}(z(\omega_i)) + 4\tilde{J}(z(2\omega_i))\right] \quad (1)$$

$$R^{ij}_{1\text{Diff}}(\omega_i) = \frac{A^{ij}_{\text{D}}}{d_{ij}D_{ij}}\left[\tilde{J}\big(z(\omega_i - \omega_j)\big) + 3\tilde{J}\big(z(\omega_i)\big) + 6\tilde{J}\big(z(\omega_i + \omega_j)\big)\right]$$

$$(2)$$

where,

$$A^{ii}_{\text{D}} = \frac{8}{45}\pi\gamma_i^4\hbar^2\left(\frac{\mu_0}{4\pi}\right)^2 n_i \quad (3a)$$

$$A^{ij}_{\text{D}} = \frac{8}{135}\pi\gamma_i^2\gamma_j^2\hbar^2\left(\frac{\mu_0}{4\pi}\right)^2 n_j \quad (3b)$$

$$\tilde{J}(z) = \frac{1 + \frac{5}{8}z + \frac{z^2}{8}}{1 + z + \frac{z^2}{2} + \frac{z^3}{6} + \frac{z^5}{81} + \frac{z^6}{648}} \quad (4)$$

The subscripts i and j refer to the proton and fluorine, respectively. $\omega = 2\pi\nu_0$, ν_0 is the Larmor frequency and $(\omega_i) \equiv \sqrt{2\omega_i d_{ij}^2/D_{ij}}$. The sum of the self-diffusion coefficients of the pair of molecules involved in the intermolecular interaction, D_i and D_j, respectively, gives the relative diffusion

This journal is © the Owner Societies 2025

Phys. Chem. Chem. Phys., 2025, **27**, 2462–2472 | **2463**

coefficient, D_{ij}. Here, d_{ij} is the closest distance between two nuclei located in different molecules, n_i is the nuclear density, $\hbar$ is Plank's constant divided by 2π, μ_0 is the vacuum magnetic permeability and γ_i is the nuclear gyromagnetic ratio.

Additionally, isotropic molecular rotations with an average correlation time were assumed as a first approximation. Then, the contribution of molecular rotations to the longitudinal relaxation rate is given by:[46,50]

$$R_{1\mathrm{Rot}}^{ii}(\omega_i) = A_\mathrm{R}\left[\frac{\tau_\mathrm{R}}{1 + (\omega_i)^2\tau_\mathrm{R}^2} + \frac{4\tau_\mathrm{R}}{1 + (2\omega_i)^2\tau_\mathrm{R}^2}\right] \quad (5)$$

where A_R is the corresponding amplitude reflecting the strength of the relevant ^{1}H–^{1}H (^{19}F–^{19}F) dipolar interactions and is given as follows:

$$A_\mathrm{R} = \frac{3}{10}\gamma_i^4\hbar^2\left(\frac{\mu_0}{4\pi}\right)^2\frac{1}{r_i^6} \quad (6)$$

Here r_i is the effective ^{1}H–^{1}H (^{19}F–^{19}F) distance between two nuclei located in the same molecule, and τ_R is the average rotational correlation time. τ_R is a characteristic time connected to molecular rotations. In the case of ILs, it represents a characteristic time for rotations of the ions as a whole. The shorter it is, the faster the molecular reorientations occur.

Finally, if the translational and rotational contributions are assumed uncoupled and dominant in different time scales, the total longitudinal relaxation rate can be expressed as:

$$R_{1\mathrm{IL}}(\omega) = R_{1\mathrm{Rot}}^{ii}(\omega) + R_{1\mathrm{Diff}}^{ii}(\omega) + R_{1\mathrm{Diff}}^{ij}(\omega) \quad (7)$$

This equation describes the hydrogen and fluorine relaxation rate dispersions of the ILs investigated in this paper. It is

worth mentioning that this model has been successfully employed to describe relaxation profiles of ILs in previous works.[17,20,31]

Experimental section

Materials and sample preparation

The ILs were synthesized as described previously (see ref. 16 for details). In all, seven ILs were studied. They were composed of the cation 1-butyl-3-methylimidazolium ([BMIM]$^+$) and the following anions: (methylsulfonyl)(2,2,2-trifluoroacetyl)imide ([NMsTFA]$^-$), acetyl((trifluoromethyl)sulfonyl)imide ([NTfAc]$^-$), bis((trifluoromethane)sulfonyl)methanide ([CHTf$_2$]$^-$ or [TFSM]$^-$), bis((perfluoroethyl)sulfonyl)imide ([NPf$_2$]$^-$ or [BETI]$^-$), bis(fluorosulfonyl)imide ([NFs$_2$]$^-$ or [FSI]$^-$), 6-membered cyclic perfluoroalkylbis(sulfonyl)imide ([6cPFSI]$^-$) and tetracyanoborate ([B(CN)$_4$]$^-$). Schematics of the ions are shown in Fig. 1. [B(CN)$_4$]$^-$ is a weakly coordinating anion that possesses only one conformer (rigid anion) and it was included to compare with the fluorinated rigid anion [6cPFSI]$^-$, which is covalently locked into the *cis* conformer. The [BMIM][TFSI] was included as a reference.

Self-diffusion coefficient measurements using PFG-NMR

Details of the pulse sequence, parameters and fitting procedure for the ^{1}H and ^{19}F self-diffusion coefficients (D) can be found in a former publication by Rauber *et al.*[51] To determine the individual self-diffusion coefficients of the ILs, NMR spectra were recorded in argon-filled, sealed NMR tubes using an AVANCE II 400 spectrometer (Bruker, Billerica, USA) with a 5 mm BBFO probe. The experiments were conducted at 25, 35,
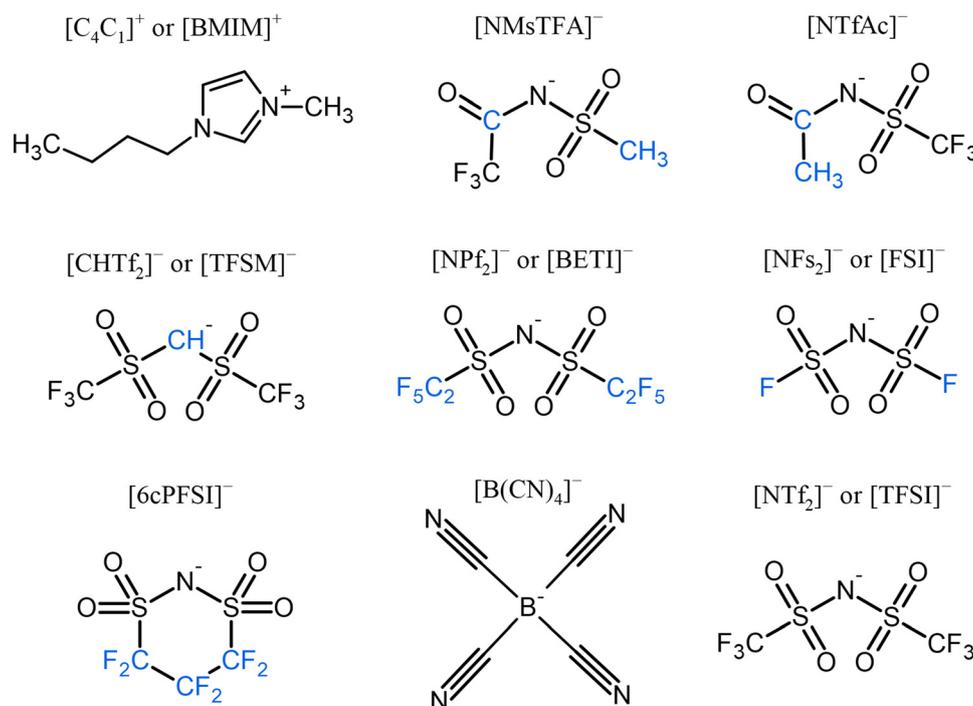

Fig. 1 Molecular structure of the cation [BMIM]$^+$ and the anions of the studied ILs. The [TFSI]$^-$ anion is included for comparison purposes and the chemical modifications in the anions are highlighted in blue color.

2464 | *Phys. Chem. Chem. Phys.*, 2025, **27**, 2462–2472

This journal is © the Owner Societies 2025

and 55 °C. For each self-diffusion coefficient determination, 16 spectra were recorded, with 16 scans each. The self-diffusion coefficients D were calculated by fitting the echo signal decay with the Stejskal-Tanner equation:[52] $I = I_0 \exp[-(\delta G \gamma)^2 (\Delta - \delta/3)D]$, where I is the amplitude of the attenuated echo signal, I_0 is the initial intensity, G is the gradient strength, δ is the gradient pulse duration, Δ is the diffusion time, and γ is the ^{1}H or ^{19}F gyromagnetic ratio.

Considering the chemical structure of the cation and anions in our samples (Fig. 1), studying the self-diffusion of ^{1}H and ^{19}F is equivalent to studying the diffusion of $[BMIM]^+$ and the anions that contain ^{19}F, respectively. For anions containing hydrogen, the signals in the ^{1}H spectra could be separated from the ones of the cation as a high resolution NMR spectrometer was used. The diffusion coefficient of $[B(CN)_4]^-$ could not be measured because it is fluorine-free and the large electric quadrupole moment of the ^{11}B nucleus yields too rapid relaxation to measure $[B(CN)_4]^-$ ion diffusion using PFG methods.

Longitudinal relaxation rate dispersion measurements using FFC-NMR relaxometry

^{1}H (cation) and ^{19}F (anion) relaxation dispersion profiles of the ILs were measured using a Spinmaster FFC2000 CDC Relaxometer (Stelar; Mede, Italy), which can electronically switch the magnetic field from an initial strong polarization magnetic field to the desired relaxation field at which the nuclear spins are allowed to relax during a time τ and T_1 is measured.[27,28,45] The NMR signal is detected after switching to a higher magnetic field (the acquisition field) and applying a $\pi/2$ radio frequency pulse. The fast-switching field cycles along with strong polarization and acquisition fields are necessary to obtain a better signal-to-noise ratio (S/N).[27,45]

IL samples of 1 mL were packed into standard 10 mm NMR tubes under an argon atmosphere. For all seven samples, the polarization and acquisition fields were set to 0.353 T (15 MHz for ^{1}H Larmor frequency) and 0.378 T (16.3 MHz for ^{1}H Larmor frequency), respectively. For each relaxation dispersion profile, 20 data points were collected. The field slew rate was 13 MHz ms^{-1} and the switching time was 3 ms. Depending on the S/N, a total of 4 to 32 signal scans were taken at each delay τ and frequency. Except for $[BMIM][B(CN)_4]$, for each IL, the cation (^{1}H relaxation) and anion (^{19}F relaxation) dispersion data were collected at 25 °C and 55 °C. The Stelar variable temperature controller was used to control the temperature of the samples within ±1 °C. The anion of $[BMIM][B(CN)_4]$ is fluorine-free, therefore collection of anion dispersion data was not possible. Relaxation dispersion curves were modeled using a previously discussed methodology.[20,53]

Results and discussion

Translational diffusion of ions

^{1}H and ^{19}F self-diffusion coefficients (D) of $[BMIM]^+$ and the anions that contain ^{19}F, measured using PFG-NMR, as a function of temperature are shown in Fig. S1(a) and (b) (ESI†),

respectively, and values are tabulated in Table S1 in the ESI.† It can be seen that they follow a linear behavior in the Arrhenius plots. Signal attenuation profiles in all measurements were at least 90% and experimental uncertainties were typically less than 4% and within the size of the data points.

As expected, the diffusion coefficients of cations and anions increase with temperature, aligning with decreasing IL's viscosity. Furthermore, for all ILs, the cation diffuses faster than the anion at all temperatures. This observation is consistent with the general trend noted in the literature regarding the self-diffusion coefficients of ILs.[17,21,25,35,54] Fig. 2, which shows the D values *versus* the viscosity at 25 °C, provides a good example of this behavior, and except for the $[B(CN)_4]^-$ anion, it is attributed to the smaller molecular weight of the $[BMIM]^+$ cation compared to the anions. In terms of the anion type, the behavior observed for both the cation and anion D values is as follows: $[BMIM][B(CN)_4] > [BMIM][FSI] > [BMIM][TFSI] > [BMIM][BETI] > [BMIM][NTfAc] \approx [BMIM][TFSM] > [BMIM][6cPFSI] > [BMIM][NMsTFA]$. Coincidentally, this trend is like that of the viscosity data;[16] namely, as the IL's viscosity increases, the diffusion coefficient values decrease (Fig. 2). For instance, at 25 °C, the viscosity η of $[BMIM][FSI]$ is 33.1 mPa s and the diffusion constants are $D_{BMIM} = 4.2 \times 10^{-11}$ m^2 s^{-1} and $D_{FSI} = 4.1 \times 10^{-11}$ m^2 s^{-1}; meanwhile for the more viscous $[BMIM][NMsTFA]$ ($\eta = 288.3$ mPa s), these values are $D_{BMIM} = 5 \times 10^{-12}$ m^2 s^{-1} and $D_{NMsTFA} = 4.1 \times 10^{-12}$ m^2 s^{-1}.

Since viscosity is expected to be affected by ion size and shape, molecular mass, conformational flexibility and the magnitude of interaction between the cation and anion,[15] the results can be analyzed based on these criteria. In terms of anion size and similarity in structure (and shape) for $[FSI]^-$, $[TFSI]^-$, and $[BETI]^-$, we see that size is the determining factor. This is further supported by the similarities in both basicity and conformational flexibility[16] for the three anions. A comparison of the
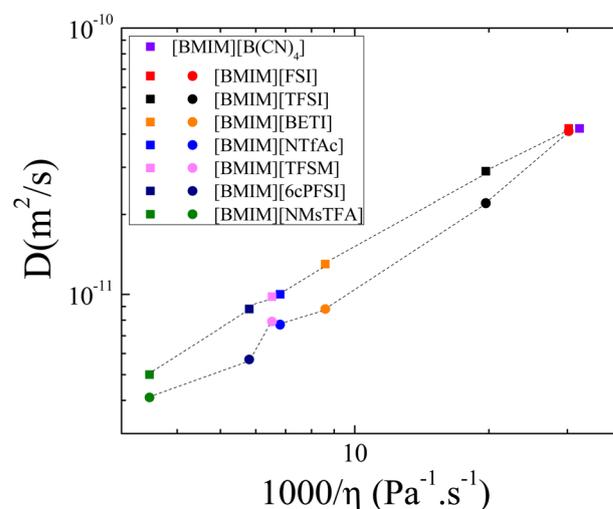

Fig. 2 Diffusion coefficients of $[BMIM]^+$ (squared symbols) and the corresponding anion (circular symbols) as a function of fluidity (inverse of viscosity η), at 25 °C. Viscosity values were taken with permission from ref. 16. The dashed lines are guides to the eye.

This journal is © the Owner Societies 2025

Phys. Chem. Chem. Phys., 2025, **27**, 2462–2472 | **2465**

[TFSI]⁻ and [TFSM]⁻ ILs highlights the effect of flexibility. As shown in Table S1 (ESI†), at 25 °C, the D values for the cation and anions are $D_{BMIM} = 28.5 \times 10^{-12}$ m² s⁻¹ and $D_{TFSI} = 21.6 \times 10^{-12}$ m² s⁻¹ for [BMIM][TFSI], and $D_{BMIM} = 9.8 \times 10^{-12}$ m² s⁻¹ and $D_{TFSM} = 7.9 \times 10^{-12}$ m² s⁻¹ for [BMIM][TFSM] respectively, which is a factor of ∼3. This difference is like that observed in the previously reported viscosity measurements,[16] which showed a value of 153 mPa s for [BMIM][TFSM] and 51 mPa s for [BMIM][TFSI] at 25 °C. Considering the almost identical masses (280 g mol⁻¹ for [TFSI]⁻ and 279 g mol⁻¹ for [TFSM]⁻) of the two anions and similarity in structure, the difference in D and viscosity can be attributed almost exclusively to flexibility. In the previous study,[16] *ab initio* simulations of the potential energy surfaces showed a rigid separated localized landscape for the S–N–S–C dihedral angles of the [TFSM]⁻ anion, compared to a delocalized and well-connected one for the [TFSI]⁻ anion. Another example of the role of flexibility is through the comparison of the [NMsTFA]⁻ and [NTfAc]⁻ ILs. As shown in Fig. 1, they have identical mass, and their structures differ only in the placement of the terminal CF₃ and CH₃ groups. From the D results, we can surmise that the flexibility of the [NTfAc]⁻ anion is greater compared to [NMsTFA]⁻. This deduction is supported by potential energy surface simulations of the S–N–S–C dihedral angles,[16] which show a wide range of values for the [NTfAc]⁻ anion compared to [NMsTFA]⁻.

Relaxation rate dispersions

The ¹H and ¹⁹F dispersion profiles for the studied ILs at 25 °C are presented in Fig. 3(a) and (b), respectively. The size of the data points covers experimental uncertainties of typically less than 6%. It is worth mentioning that considering the chemical structure of the cation and anions in our samples, studying the relaxation rate of ¹H and ¹⁹F is equivalent to studying molecular dynamics of [BMIM]⁺ and the corresponding anions (if they have fluorine), respectively. Furthermore, as mentioned in the theory section, the R_1 values reported are average values rather than specific to individual sites of the ions, and for the physical parameters obtained from modeling, the relaxation profiles are also averaged.

As shown in Fig. 3(a), ¹H relaxation rates R_1 follow this trend: [BMIM][NMsTFA] > [BMIM][NTfAc] ≈ [BMIM][6cPFSI] > [BMIM][TFSM] > [BMIM][BETI] > [BMIM][FSI] > [BMIM][B(CN)₄], which is mainly governed by viscosity. This means that the less viscous the IL is, the more mobile the ions are and this is evidenced by smaller relaxation rates. It is worth mentioning that the room temperature (25 °C) is above the temperature of the T_1 minimum, hence more mobility yields smaller relaxation rates. A similar trend is observed at 55 °C as shown in Fig. S2 in the ESI† and for the ¹⁹F relaxation profiles at 25 °C (Fig. 3(b)) and 55 °C (Fig. S3, ESI†). For instance, the fastest relaxation of [BMIM][NMsTFA] and the slowest relaxation of [BMIM][B(CN)₄] correlate with these being the most and least viscous ILs, respectively.

The general behaviors of the relaxation profiles are more frequency dependence at 25 °C and weakening of the dispersion at 55 °C. As previously mentioned, this pattern has also
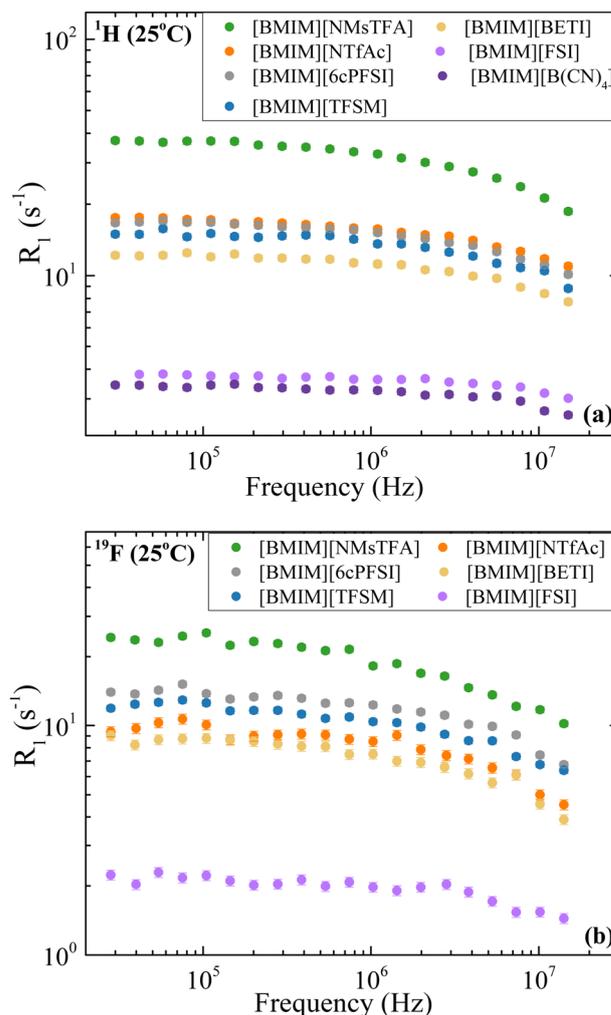

Fig. 3 (a) ¹H ([BMIM]⁺) and (b) ¹⁹F (anion) relaxation rate dispersions for [BMIM][NMsTFA], [BMIM][NTfAc], [BMIM][6cPFSI], [BMIM][TFSM], [BMIM]-[BETI], [BMIM][FSI] and [BMIM][B(CN)₄], at 25 °C.

been observed for other ILs.[17,18,20,21,25,30–40] At 25 °C, the cations display less frequency dependence compared with the anions (Fig. 3), suggesting that the dynamics of the anions are more influenced by the environment. Specifically, within the evaluated frequency range, the R_1 values for cations change by factors of approximately 1.3 to 1.9, while for anions, the change ranges from 1.6 to 2.4.

The model given by Eqn (7) was used to analyze the ¹H and ¹⁹F relaxation profiles for all ILs, at 25 °C and 55 °C. All the involved physical parameters in this model were estimated from data fitting by fixing them within their most probable intervals obtained from the literature, except for diffusion coefficient values, which were taken from our PFG-NMR diffusion measurements (Fig. S1, ESI†). All the fitting parameters for the following graphs are included in Tables S2 and S3 in the ESI.† The obtained fitting curves for [BMIM][TFSM] at 25 °C are shown in Fig. 4(a) and (b) for ¹H and ¹⁹F relaxation, respectively, where a good agreement with data can be observed within the experimental uncertainties. The fitting curves for the
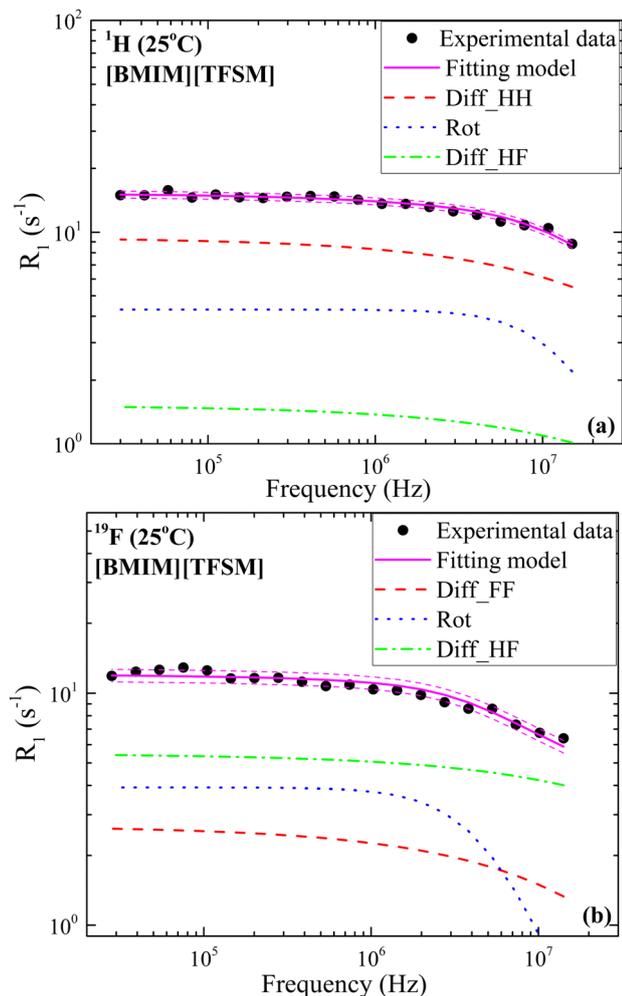
Fig. 4 (a) ^{1}H and (b) ^{19}F relaxation rate dispersions for [BMIM][TFSM] and their corresponding fittings using the model given by eqn (7), recorded at 25 °C. Additionally, rotational contribution (Rot), homonuclear (Diff_HH/Diff_FF), and heteronuclear (Diff_HF) translational contributions are shown. Magenta dashed lines represent the fitting error. Frequencies are ^{1}H and ^{19}F Larmor frequencies in (a) and (b), respectively.

Fig. 5 Average rotational time of [BMIM]$^+$ (squared symbols) and the corresponding anions (circular symbols) that contain ^{19}F in their chemical structures ([FSI]$^-$, [BETI]$^-$, [NTfAc]$^-$, [TFSM]$^-$, [6cPFSI]$^-$ and [NMsTFA]$^-$) as a function of viscosity, at 25 °C. Viscosity values were taken with permission from ref. 16. Rotational times of [BMIM]$^+$ and [TFSI]$^-$ in [BMIM][TFSI] are included for comparison purposes and are taken with permission from ref. 20. The dashed lines are guides to the eye.

Molecular rotational times τ_R of [BMIM]$^+$ and the corresponding anions ([FSI]$^-$, [BETI]$^-$, [NTfAc]$^-$, [TFSM]$^-$, [6cPFSI]$^-$ and [NMsTFA]$^-$) as a function of viscosity at 25 °C are presented in Fig. 5. Uncertainties were typically less than 6% and usually within the size of the data points. It is observed that for all ILs, [BMIM]$^+$ rotates as a whole faster than the anions due to the smaller molecular weight of the cation. It is worth mentioning that in this work, we are interested in rotational motions of the ions as a whole instead of focusing on specific parts of them. Therefore, the average rotational times derived from modeling the relaxation profiles are more suitable for our study instead of using local, site-specific rotational motion.

The rotational time values do not show a clear trend as viscosity increases, contrasting with the distinct trend observed for the diffusion coefficients shown in Fig. 2. This suggests that the rotational time is more sensitive to the structure of the ions. Although the anion's rotational motion slows down at the highest viscosity, this is insufficient to draw strong conclusions. The absence of a clear trend in τ_R as a function of viscosity is due to the competing effects of many variables, such as mass, fluorination, and flexibility of ions in these ILs. To better understand the impact of each variable on the ion rotational dynamics, smaller groups of ILs are compared in the following section.

Effect of conformational flexibility, fluorination, and mass on molecular motions of ions

In this section, the investigated ILs are grouped to analyze the effect of conformational flexibility, fluorination, and mass of the anions on the translational and rotational motions of both the cation and anion. The groups are defined as presented in Table 1 and all of them have [BMIM][TFSI] as a reference. [TFSI]$^-$ has a molecular weight of 280 g mol^{-1}, six fluorines,

other ILs are given in the ESI† (Fig. S4–S16). In Fig. 4(a), it is seen that ^{1}H relaxation is dominated by homonuclear translational diffusion (Diff_HH) in the whole frequency range. Additionally, the rotational contribution is quite important in the same frequency range but the heteronuclear translational diffusion contribution (Diff_HF) is very small because of the lower density of fluorine compared to hydrogen (six *vs.* fifteen per ion pair). On the other hand, in the case of ^{19}F relaxation, the heteronuclear diffusion contribution is the dominant one as shown in Fig. 4(b). A similar behavior is observed for all other ILs as displayed in Fig. S4–S16 (ESI†), except for ^{19}F relaxation for [BMIM][6cPFSI] (Fig. S15, ESI†) in which the rotational contribution is the dominant relaxation mechanism over almost the whole frequency range. This should be connected to the rigid (cyclic) structure of [6cPFSI]$^-$ which makes molecular rotation a very efficient relaxation mechanism.
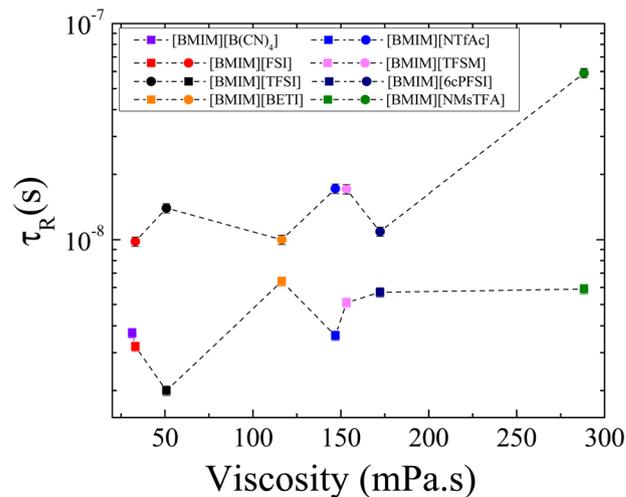
This journal is © the Owner Societies 2025

Phys. Chem. Chem. Phys., 2025, **27**, 2462–2472 | **2467**

Table 1 Groups of ILs to experimentally investigate the effects of conformational flexibility, fluorination, and mass of the anion on the ILs' dynamics

Group	
A: Flexibility	[BMIM][TFSI]
	[BMIM][NMsTFA]
	[BMIM][NTfAc]
B: Flexibility	[BMIM][TFSI]
	[BMIM][TFSM]
C: Fluorination and mass	[BMIM][TFSI]
	[BMIM][FSI]
	[BMIM][BETI]
D: Fluorination and flexibility	[BMIM][TFSI]
	[BMIM][6cPFSI]
	[BMIM][B(CN)$_4$]

and is considered flexible due to its ability to quickly switch between *cis* and *trans* conformers. The reason for this is that the energy barrier between these two conformers is small, specifically lower than 15 kJ mol^{-1}. As done in a previous study,[16] an anion is considered flexible in this paper if its conformers are separated by energy barriers lower than 15 kJ mol^{-1}.

Group A contains the anions [NMsTFA]$^-$ and [NTfAc]$^-$, which have identical molecular weights (190 g mol^{-1}) and the same degree of fluorination (3F), but the different relative positions of the CH$_3$ and CF$_3$ groups (Fig. 1) lead to a difference in conformational flexibility.[16] Specifically, [NMsTFA]$^-$ is rigid, while [NTfAc]$^-$ is flexible. Fig. 6 shows that both the cation and anion have faster translational and rotational motions in [BMIM][NTfAc] than in [BMIM][NMsTFA]. This demonstrates and reaffirms that when the anion is flexible, there is reduced interaction between the cation and the anion. Therefore, the IL is less viscous ($\eta^{[BMIM][NTfAc]}$ = 146.9 mPa s *vs.* $\eta^{[BMIM][NMsTFA]}$ = 288.3 mPa s at 25 °C), and molecular motions are faster. It is worth noting that [TFSI]$^-$ is the heaviest anion in this group due to its high degree of fluorination. However, [BMIM][TFSI] is the IL with the fastest dynamics due to its conformational flexibility. This example illustrates that the impact of mass on transport properties is minimal when there is a substantial difference in flexibility.[16] As mentioned previously, the increased flexibility of [NTfAc]$^-$ compared to [NMsTFA]$^-$ is supported by potential energy surface simulations[16] showing the breadth of the S–N–S–C dihedral angles.

On the other hand, group B consists of two anions, [TFSI]$^-$ and [TFSM]$^-$, which have similar molecular weights of 280 and 279 g mol^{-1}, respectively. They also have the same degree of fluorination (6F). However, the difference in their conformational flexibility[16] is due to the replacement of the flexible S–N–S bond by S–CH–S (as shown in Fig. 1). Fig. 7 displays that the IL with the flexible anion [TFSI]$^-$ has faster translational and rotational motions for both the cation and anion. This result highlights the significant influence of flexibility on the movement of ions.

Increasing the fluorination of the anion results in a corresponding increase in mass and volume. Since conformational flexibility does not change considerably in group C, the size of the anion becomes more important in comparison. This group
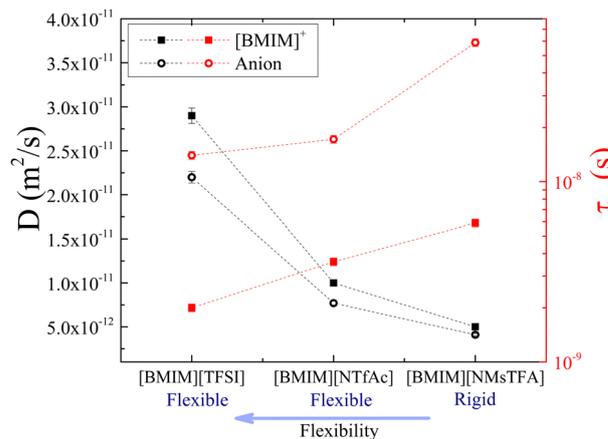

Fig. 6 Diffusion coefficients (black symbols) and rotational times (red symbols) of [BMIM]$^+$ (squared solid symbols) and the corresponding anion (circular hollow symbols) in the three ILs of group A, at 25 °C. Rotational times of [BMIM]$^+$ and [TFSI]$^-$ in [BMIM][TFSI] are taken with permission from ref. 20. Dashed lines are guides to the eye.

comprises the flexible anions [FSI]$^-$ and [BETI]$^-$, which have different molecular weights of 180 and 380 g mol^{-1}, respectively. They have different levels of fluorination as well, with one having two fluorine atoms and the other having ten (as shown in Fig. 1). Although the translational motion of the cation and anion in [BMIM][FSI] is faster, there is no straight trend for rotational motion, as presented in Fig. 8. It is observed that the rotational motion of the cation is influenced by the degree of fluorination and molecular mass of the anion, while the molecular reorientations of the anions remain nearly unaffected. Since the degree of fluorination also affects the negative charge delocalization and the anion's coordination affinity, the rotational motion result is likely an illustration of the competing influences of coordination affinity and mass on the ion's rotational dynamics. The similarity in D values for the cation and anion in [BMIM][FSI] is noteworthy and may be the
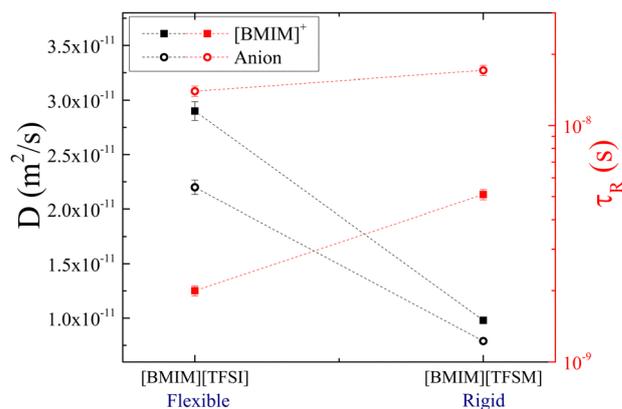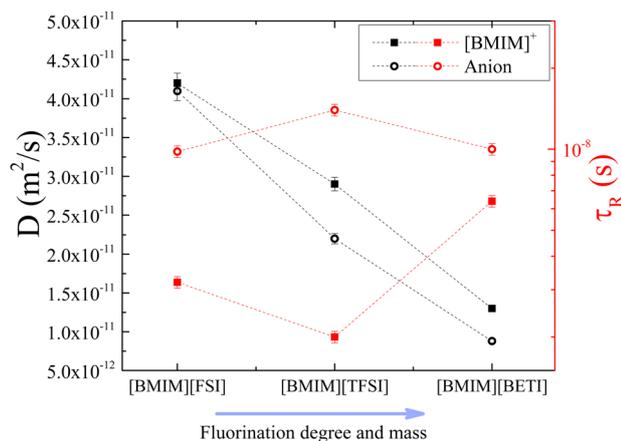

Fig. 7 Diffusion coefficients (black symbols) and rotational times (red symbols) of [BMIM]$^+$ (squared solid symbols) and the corresponding anion (circular hollow symbols) in the ILs of group B, at 25 °C. Rotational times of [BMIM]$^+$ and [TFSI]$^-$ in [BMIM][TFSI] are taken with permission from ref. 20. Dashed lines are guides to the eye.

2468 | *Phys. Chem. Chem. Phys.*, 2025, **27**, 2462–2472

This journal is © the Owner Societies 2025

Fig. 8 Diffusion coefficients (black symbols) and rotational times (red symbols) of $[BMIM]^+$ (squared solid symbols) and the corresponding anion (circular hollow symbols) in the three ILs of group C, at 25 °C. Rotational times of $[BMIM]^+$ and $[TFSI]^-$ in $[BMIM][TFSI]$ are taken with permission from ref. 20. Dashed lines are guides to the eye.

most direct evidence of greater coordination affinity from less fluorine content. Despite this, the cation still rotates faster. In the case of $[BMIM][TFSI]$, the increased fluorine content is expected to reduce this coordination affinity causing the observed acceleration in the cation rotational motion. Further increase in fluorination as in the case of the $[BETI]^-$ anion, however, makes size the more dominant factor, causing a reduction in the rotation of the $[BMIM]^+$ cation and an increase in that of the $[BETI]^-$ anion. These results suggest greater coordination between the motions of the anion and cation and are a good demonstration of the delicate and unstable balance between mass, fluorination level and flexibility.

Regarding group D, which consists of the two rigid anions $[6cPFSI]^-$ and $[B(CN)_4]^-$, the size of the anion takes relevance again since these two anions have no flexibility because they are
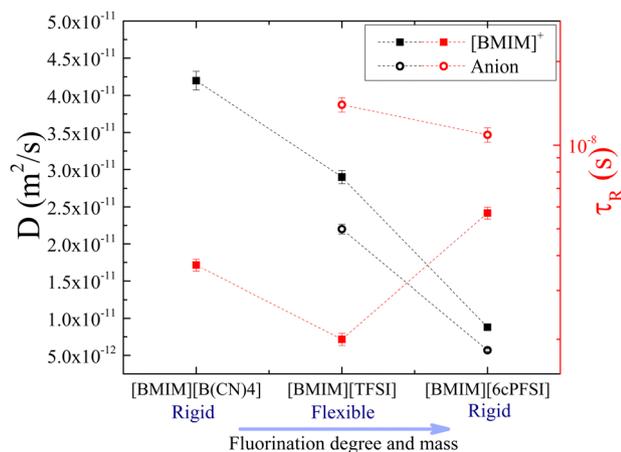

Fig. 9 Diffusion coefficients (black symbols) and rotational times (red symbols) of $[BMIM]^+$ (squared solid symbols) and the corresponding anion (circular hollow symbols) in the three ILs of group D, at 25 °C. Rotational times of $[BMIM]^+$ and $[TFSI]^-$ in $[BMIM][TFSI]$ are taken with permission from ref. 20. Dashed lines are guides to the eye.

locked into one conformer. They possess different molecular weights of 292 and 115 g mol^{-1} and degrees of fluorination of six and zero, respectively. As expected, due to the larger size of $[6cPFSI]^-$, translational and rotational motions of the cation in $[BMIM][6cPFSI]$ are slower compared to $[BMIM][B(CN)_4]$, as shown in Fig. 9. It was not possible to determine the translational diffusion coefficient and rotational time for $[B(CN)_4]^-$, as mentioned earlier. On the other hand, both $[6cPFSI]^-$ and $[TFSI]^-$ have similar molecular weights (292 vs. 280 g mol^{-1}) and six fluorine atoms, but they differ significantly in flexibility and as a direct consequence, coordination affinity. As displayed in Fig. 9, the cation and anion's translational dynamics are faster in $[BMIM][TFSI]$ compared to $[BMIM][6cPFSI]$, but their rotational motions exhibit the dominance of reduced cation–anion coordination affinity over size. In $[BMIM][6cPFSI]$, the molecular reorientations of $[BMIM]^+$ slow down, while the rotations of the anion slightly accelerate in comparison to $[BMIM][TFSI]$. These effects may be an indication of the increased coordination between the $[BMIM]^+$ cation and $[6cPFSI]^-$ anion caused by the anion's rigidity. Because of this coordination, the cation and anion rotate slower and faster, respectively, compared to $[BMIM][TFSI]$.

Conclusions

In this work, FFC-NMR relaxometry and PFG-NMR techniques have been combined to study the rotational and translational dynamics of the cations and anions in six ILs composed of $[BMIM]^+$ and chemically modified analogs of $[TFSI]^-$, at different temperatures. The diffusion coefficients obtained from PFG-NMR measurements provided an input used to fit the FFC data successfully, which validates the models used to describe the relaxation profiles.

The properties of mass, fluorination level, flexibility and viscosity are all drivers and determinants of ion dynamics. Results show that in media where all four properties exist, the resulting ion dynamics depends on which property dominates. Unfortunately, a clear winner is oftentimes difficult to ascertain. Instead, what results is a local environment where competing properties create an unstable equilibrium that drives ions dynamics. After grouping the ILs, it was observed that the rotational and translational motions of the cations and anions followed a trend. If there is a significant difference in conformational flexibility between the compared ILs, the IL with a larger anion's conformational flexibility will have faster dynamics, regardless of the mass and fluorination level of the anions. The benefit of greater flexibility is a reduction in the local interactions such as electrostatic and hydrogen bonding ones. This reduction in turn creates reduced friction that will facilitate faster ion dynamics.

However, if the flexibility of the anions in the same group is similar, the competing influences of fluorination (coordination affinity) and mass will determine which IL has faster dynamics. As the mass ergo size of the anion increases, the local interactions and correspondingly the viscosity will increase. These in

This journal is © the Owner Societies 2025

Phys. Chem. Chem. Phys., 2025, **27**, 2462–2472 | **2469**

turn will reduce ion dynamics. Similarly, as the fluorination level increases over this flexible or inflexible anion, so does its ability to coordinate with counter-ions. This coordinating effect can be countered by the degree of charge delocalization over the anion which also depends on its size. Overall, the picture that emerges is one in which efficient ion dynamics depends on the delicate and unstable balance between mass, fluorination level, viscosity and flexibility.

Despite these competing properties, the most influential appears to be flexibility. This may be because greater flexibility reduces ion–ion interactions thereby enhancing dynamics. This is supported by the higher self-diffusion coefficients for both the anions and cations in ILs containing anions with greater flexibility, irrespective of mass, and fluorination levels. The rotational motions of ions are also significantly impacted by anion's flexibility.

Author contributions

Tawhid Pranto: data curation, formal analysis (FFC-NMR), investigation (FFC-NMR), validation, visualization, and writing – original draft. Carla C. Fraenza: conceptualization, data curation, methodology, project administration, supervision, visualization, writing – original draft, and writing – review and editing. Frederik Philippi: conceptualization, investigation (syntheses), resources, and writing – review and editing. Daniel Rauber: formal analysis (PFG-NMR), investigation (syntheses, PFG-NMR), resources, and writing – review and editing. Christopher W. M. Kay: funding acquisition and writing – review and editing. Tom Welton: funding acquisition and writing – review and editing. Steven Greenbaum: funding acquisition and writing – review and editing. Sophia Suarez: conceptualization, funding acquisition, project administration, supervision, writing – original draft, and writing – review and editing.

Data availability

All experimental and fitting data associated with this publication are stored in hard drives at the respective universities and are accessible to the science community through requests made to authors.

Conflicts of interest

There are no conflicts to declare.

Acknowledgements

References

1 M. Freemantle, *An introduction to ionic liquids*, Royal Society of chemistry, 2010.

2 T. Welton, Ionic liquids: a brief history, *Biophys. Rev.*, 2018, **10**, 691–706.

3 A. Eftekhari, Y. Liu and P. Chen, Different roles of ionic liquids in lithium batteries, *J. Power Sources*, 2016, **334**, 221–239.

4 M. Watanabe, M. L. Thomas, S. Zhang, K. Ueno, T. Yasuda and K. Dokko, Application of ionic liquids to energy storage and conversion materials and devices, *Chem. Rev.*, 2017, **117**, 7190–7239.

5 T. Rüther, A. I. Bhatt, A. S. Best, K. R. Harris and A. F. Hollenkamp, Electrolytes for lithium (sodium) batteries based on ionic liquids: highlighting the key role played by the anion, *Batteries Supercaps*, 2020, **3**, 793–827.

6 K. Liu, Z. Wang, L. Shi, S. Jungsuttiwong and S. Yuan, Ionic liquids for high performance lithium metal batteries, *J. Energy Chem.*, 2020, **59**, 320–333.

7 T. Stettner and A. Balducci, Protic ionic liquids in energy storage devices: Past, present and future perspective, *Energy Storage Mater.*, 2021, **40**, 402–414.

8 H. Niu, L. Wang, P. Guan, N. Zhang, C. Yan, M. Ding, X. Guo, T. Huang and X. Hu, Recent advances in application of ionic liquids in electrolyte of lithium ion batteries, *J. Energy Storage*, 2021, **40**, 102659.

9 X. Tang, S. Lv, K. Jiang, G. Zhou and X. Liu, Recent development of ionic liquid-based electrolytes in lithium-ion batteries, *J. Power Sources*, 2022, **542**, 231792.

10 H. Srinivasan, V. K. Sharma, R. Mukhopadhyay and S. Mitra, Solvation and transport of lithium ions in deep eutectic solvents, *J. Chem. Phys.*, 2020, **153**, 104505.

11 Q.-K. Zhang, X.-Q. Zhang, H. Yuan and J.-Q. Huang, Thermally Stable and Nonflammable Electrolytes for Lithium Metal Batteries: Progress and Perspectives, *Small Sci.*, 2021, **1**, 2100058.

12 Y. An, X. Han, Y. Liu, A. Azhar, J. Na, A. K. Nanjundan, S. Wang, J. Yu and Y. Yamauchi, Progress in Solid Polymer Electrolytes for Lithium-Ion Batteries and Beyond, *Small*, 2022, **18**, 2103617.

13 G. Yu, D. Zhao, L. Wen, S. Yang and X. Chen, Viscosity of ionic liquids: Database, observation, and quantitative structure-property relationship analysis, *AIChE J.*, 2012, **58**, 2885–2899.

14 S. Jiang, Y. Hu, Y. Wang and X. Wang, Viscosity of typical room-temperature ionic liquids: a critical review, *J. Phys. Chem. Ref. Data*, 2019, **48**, 033101.

2470 | *Phys. Chem. Chem. Phys.*, 2025, **27**, 2462–2472

This journal is © the Owner Societies 2025

15 S. Tsuzuki, Factors controlling the diffusion of ions in ionic liquids, *Chem. Phys. Chem.*, 2012, **13**, 1664–1670.

16 F. Philippi, D. Rauber, O. Palumbo, K. Goloviznina, J. McDaniel, D. Pugh, S. Suarez, C. C. Fraenza, A. Padua, C. W. Kay and T. Welton, Flexibility is the key to tuning the transport properties of fluorinated imide-based ionic liquids, *Chem. Sci.*, 2022, **13**, 9176–9190.

17 A. O. Seyedlar, S. Stapf and C. Mattea, Dynamics of the ionic liquid 1-butyl-3-methylimidazolium bis (trifluoromethylsulphonyl) imide studied by nuclear magnetic resonance dispersion and diffusion, *Phys. Chem. Chem. Phys.*, 2015, **17**, 1653–1659.

18 K. Pilar, A. Rua, S. N. Suarez, C. Mallia, S. Lai, J. Jayakody, J. L. Hatcher, J. F. Wishart and S. Greenbaum, Investigation of dynamics in BMIM TFSA ionic liquid through variable temperature and pressure NMR relaxometry and diffusometry, *J. Electrochem. Soc.*, 2017, **164**, H5189.

19 M. Becher, E. Steinrücken and M. Vogel, On the relation between reorientation and diffusion in glass-forming ionic liquids with micro-heterogeneous structures, *J. Chem. Phys.*, 2019, **151**, 194503.

20 N. K. Jayakody, C. C. Fraenza, S. G. Greenbaum, D. Ashby and B. S. Dunn, NMR relaxometry and diffusometry analysis of dynamics in ionic liquids and ionogels for use in lithium-ion batteries, *J. Phys. Chem. B*, 2020, **124**, 6843–6856.

21 V. Overbeck, B. Golub, H. Schroeder, A. Appelhagen, D. Paschek, K. Neymeyr and R. Ludwig, Probing relaxation models by means of Fast Field-Cycling relaxometry, NMR spectroscopy and molecular dynamics simulations: Detailed insight into the translational and rotational dynamics of a protic ionic liquid, *J. Mol. Liq.*, 2020, **319**, 114207.

22 J. B. Beckmann, D. Rauber, F. Philippi, K. Goloviznina, J. A. Ward-Williams, A. J. Sederman, M. D. Mantle, A. Pádua, C. W. Kay and T. Welton, Molecular Dynamics of Ionic Liquids from Fast-Field Cycling NMR and Molecular Dynamics Simulations, *J. Phys. Chem. B*, 2022, **126**, 7143–7158.

23 S. Zhang, N. Sun, X. He, X. Lu and X. Zhang, Physical properties of ionic liquids: database and evaluation, *J. Phys. Chem. Ref. Data*, 2006, **35**, 1475–1517.

24 J. G. McDaniel, C. Y. Son and A. Yethiraj, Ab initio force fields for organic anions: Properties of [BMIM][TFSI],[B-MIM][FSI], and [BMIM][OTF] ionic liquids, *J. Phys. Chem. B*, 2018, **122**, 4101–4114.

25 D. Kruk, R. Meier, A. Rachocki, A. Korpała, R. Singh and E. Rössler, Determining diffusion coefficients of ionic liquids by means of field cycling nuclear magnetic resonance relaxometry, *J. Chem. Phys.*, 2014, **140**, 244509.

26 R. Blundell and P. Licence, Tuning cation–anion interactions in ionic liquids by changing the conformational flexibility of the cation, *Chem. Commun.*, 2014, **50**, 12080–12083.

27 R. Kimmich and E. Anoardo, Field-cycling NMR relaxometry, *Prog. Nucl. Magn. Reson. Spectrosc.*, 2004, **44**, 257–320.

28 R. Kimmich, *Field-cycling NMR Relaxometry: Instrumentation, Model Theories and Applications*, Royal Society of Chemistry, 2018.

29 P. Conte, *Annual Reports on NMR Spectroscopy*, Elsevier, 2021, vol. 104, pp. 141–188.

30 A. Rachocki, E. Andrzejewska, A. Dembna and J. Tritt-Goc, Translational dynamics of ionic liquid imidazolium cations at solid/liquid interface in gel polymer electrolyte, *Eur. Polym. J.*, 2015, **71**, 210–220.

31 D. Kruk, M. Wojciechowski, S. Brym and R. K. Singh, Dynamics of ionic liquids in bulk and in confinement by means of 1H NMR relaxometry–BMIM-OcSO$_4$ in an SiO$_2$ matrix as an example, *Phys. Chem. Chem. Phys.*, 2016, **18**, 23184–23194.

32 A. Ordikhani Seyedlar, S. Stapf and C. Mattea, Cation dynamics in supercooled and solid alkyl methylimidazolium bromide ionic liquids, *J. Phys. Chem. B*, 2017, **121**, 5363–5373.

33 D. Kruk, M. Wojciechowski, Y. L. Verma, S. K. Chaurasia and R. K. Singh, Dynamical properties of EMIM-SCN confined in a SiO$_2$ matrix by means of 1H NMR relaxometry, *Phys. Chem. Chem. Phys.*, 2017, **19**, 32605–32616.

34 G. W. Driver, Y. Huang, A. Laaksonen, T. Sparrman, Y.-L. Wang and P.-O. Westlund, Correlated/non-correlated ion dynamics of charge-neutral ion couples: the origin of ionicity in ionic liquids, *Phys. Chem. Chem. Phys.*, 2017, **19**, 4975–4988.

35 M. Wencka, T. Apih, R. C. Korošec, J. Jenczyk, M. Jarek, K. Szutkowski, S. Jurga and J. Dolinšek, Molecular dynamics of 1-ethyl-3-methylimidazolium triflate ionic liquid studied by 1H and 19F nuclear magnetic resonances, *Phys. Chem. Chem. Phys.*, 2017, **19**, 15368–15376.

36 J. Kaszyńska, A. Rachocki, M. Bielejewski and J. Tritt-Goc, Influence of cellulose gel matrix on BMIMCl ionic liquid dynamics and conductivity, *Cellulose*, 2017, **24**, 1641–1655.

37 Z. Wojnarowska, H. Feng, M. Diaz, A. Ortiz, I. Ortiz, J. Knapik-Kowalczuk, M. Vilas, P. Verdía, E. Tojo and T. Saito, Revealing the charge transport mechanism in polymerized ionic liquids: Insight from high pressure conductivity studies, *Chem. Mater.*, 2017, **29**, 8082–8092.

38 V. Overbeck, A. Appelhagen, R. Rößler, T. Niemann and R. Ludwig, Rotational correlation times, diffusion coefficients and quadrupolar peaks of the protic ionic liquid ethylammonium nitrate by means of 1H fast field cycling NMR relaxometry, *J. Mol. Liq.*, 2021, **322**, 114983.

39 C. C. Fraenza and S. G. Greenbaum, Broadband NMR relaxometry as a powerful technique to study molecular dynamics of ionic liquids, *ChemPhysChem*, 2023, **24**, e202300268.

40 L. Kruse, A. M. Chiramel Tony, D. Paschek, P. Stange, R. Ludwig and A. Strate, Translational Dynamics of Cations and Anions in Ionic Liquids from NMR Field Cycling Relaxometry: Highlighting the Importance of Heteronuclear Contributions, *J. Phys. Chem. Lett.*, 2024, **15**, 10410–10415.

41 K. Damodaran, Recent advances in NMR spectroscopy of ionic liquids, *Prog. Nucl. Magn. Reson. Spectrosc.*, 2022, **129**, 1–27.

42 O. Borodin, W. Gorecki, G. D. Smith and M. Armand, Molecular dynamics simulation and pulsed-field gradient NMR studies of bis (fluorosulfonyl) imide (FSI) and bis

This journal is © the Owner Societies 2025

Phys. Chem. Chem. Phys., 2025, **27**, 2462–2472 | **2471**

[(trifluoromethyl) sulfonyl] imide (TFSI)-based ionic liquids, *J. Phys. Chem. B*, 2010, **114**, 6786–6798.

43 K. Ramya, P. Kumar and A. Venkatnathan, Molecular simulations of anion and temperature dependence on structure and dynamics of 1-hexyl-3-methylimidazolium ionic liquids, *J. Phys. Chem. B*, 2015, **119**, 14800–14806.

44 S. Tsuzuki, H. Matsumoto, W. Shinoda and M. Mikami, Effects of conformational flexibility of alkyl chains of cations on diffusion of ions in ionic liquids, *Phys. Chem. Chem. Phys.*, 2011, **13**, 5987–5993.

45 E. Anoardo, G. Galli and G. Ferrante, Fast-field-cycling NMR: Applications and instrumentation, *Appl. Magn. Reson.*, 2001, **20**, 365–404.

46 A. Abragam, *The principles of nuclear magnetism*, Oxford University Press, 1961.

47 Y. Ayant, E. Belorizky, J. Aluzon and J. Gallice, Calcul des densités spectrales résultant d'un mouvement aléatoire de translation en relaxation par interaction dipolaire magnétique dans les liquides, *J. Phys.*, 1975, **36**, 991–1004.

48 L. P. Hwang and J. H. Freed, Dynamic effects of pair correlation functions on spin relaxation by translational diffusion in liquids, *J. Chem. Phys.*, 1975, **63**, 4017–4025.

49 J. H. Freed, Dynamic effects of pair correlation functions on spin relaxation by translational diffusion in liquids. II. Finite jumps and independent T 1 processes, *J. Chem. Phys.*, 1978, **68**, 4034–4037.

50 N. Bloembergen, E. M. Purcell and R. V. Pound, Relaxation effects in nuclear magnetic resonance absorption, *Phys. Rev.*, 1948, **73**, 679–712.

51 D. Rauber, F. Philippi, J. Zapp, G. Kickelbick, H. Natter and R. Hempelmann, Transport properties of protic and aprotic guanidinium ionic liquids, *RSC Adv.*, 2018, **8**, 41639–41650.

52 E. O. Stejskal and J. E. Tanner, Spin diffusion measurements: spin echoes in the presence of a time-dependent field gradient, *J. Chem. Phys.*, 1965, **42**, 288–292.

53 C. C. Fraenza and E. Anoardo, Dynamical regimes of lipids in additivated liposomes with enhanced elasticity: A field-cycling NMR relaxometry approach, *Biophys. Chem.*, 2017, **228**, 38–46.

54 K. R. Harris and M. Kanakubo, Self-diffusion coefficients and related transport properties for a number of fragile ionic liquids, *J. Chem. Eng. Data*, 2016, **61**, 2399–2411.